Electric field effect in heat transfer in 2D devices

A I Volokitin[1,2] and B N J Persson[2]

[1] Samara State Technical University, Molodogvardeiskaya Str. 244, 443100 Samara, Russia
[2] Peter Grünberg Institut, Forschungszentrum Jülich, D-52425, Germany

E-mail: alevolokitin@yandex.ru

CrossMark

Abstract

We calculate heat transfer between a 2D sheet (e.g. graphene) and a dielectric in presence of a gate voltage. The gate potential induces surface charge densities on the sheet and dielectric, which results in electric field, which is coupled to the surface displacements and, as a consequence, resulting an additional contributions to the radiative heat transfer. The electrostatic and van der Waals interactions between the surface displacement result in the phonon heat transfer, which we calculate taking into account the nonlocality of these interactions. Numerical calculations are presented for heat transfer between graphene and a SiO_2 substrate.

(Some figures may appear in colour only in the online journal)

1. Introduction

At present the problem of heat transfer in 2D devices is actively discussed [1]. For example, it is important in the development of graphene transistor. Heat generation during high-density electric current flowing in graphene will increase the temperature, which can damage the device. Therefore, it is important to be able to control heat flux. Interfacial heat transfer between 2D crystal and substrate can occur via near-field radiative [2] and phonon [1, 3, 4] heat transfer.

The ability to control the electrical properties of materials underlies modern electronics. Currently, in connection with the development of new technologies related to nanoscale thermal management, energy storage and conversion, and information processing, the problem of the management of the heat transfer is being actively considered. In 2006, Li *et al* [5] proposed a thermal analogue of the field effect transistor for controlling heat transfer by phonons through solid segments, paving the way for creating blocks for processing information [6, 7] using heat flow instead of electric current. More recently the concept of thermal transistor has been expanded to noncontact systems out of thermal equilibrium [8]. In this case, heat fluxes are associated with the transmission of thermal photons from one material to another.

A radiation heat transistor consists of three elements, which by analogy with its electronic counterpart, are called source, drain and gate. Source and drain are maintained at different temperatures to create a temperature gradient. Source, being traditionally hotter than drain, emits thermal photons that transmit heat to the drain. These two solids are separated by intermediate layer made of insulator-metal phase transition material [9]. This layer acts as a gate. By adjusting the gate temperature near a critical value, it is possible radically change the heat flow obtained by drain and even enhance this flow. The device can work either at large separation (far field [10]), where heat fluxes are associated with the propagating photons, or at short distances (near field [8]), where heat is transmitted primarily by photon tunneling. Beyond modulation and heat flow amplification, these structures based on phase transition materials can be used for storage thermal energy and logical operations with thermal photons.

In this article we consider the possibility of controlling the radiative and phonon heat flux between a 2D sheet (e.g. graphene) and a dielectric substrate (e.g. SiO_2) using the field effect, similar to how it is used to control electronic properties in a graphene transistor [11].The gate voltage induces surface charge densities on the sheet and dielectric. The thermal fluctuations of the displacements of the charged surfaces give

rise to an additional contribution to the fluctuating electromagnetic field which result in an additional contributions to the radiative heat transfer. The electrostatic and van der Waals interactions between surface displacements produce the phonon heat transfer. In contrast to our previous 'spring' model [3], now we take into account the nonlocality in these interactions. The methodological approach that is used in this article was previously used to calculate heat transfer between 3D metals [12, 13]. The electrostatic and van der Waals phonon heat transfer was also recently studied in reference [14] using different approach.

2. Theory

2.1. Radiative heat transfer

Consider a 2D sheet (e.g. graphene) located in the (x, y)-plane at $z = 0$ and separated from a dielectric slab with thickness h (e.g. SiO$_2$) by vacuum gap with thickness d (figure 1). The application of the gate voltage (V_G) induces a surface charge density on the sheet, $\sigma_g = ne = E_0/4\pi$, where n is the concentration of the free charge carries in the sheet, E_0 is the electric field in the vacuum gap between the sheet and dielectric. In general, the application of a gate voltage (V_G) creates an electrostatic potential difference φ between the graphene and the gate electrode, and the addition of charge carriers leads to a shift in the Fermi level (E_F). Therefore V_G is given by [15]

$$V_G = \frac{E_F}{e} + \varphi \qquad (1)$$

with E_F/e being determined by the chemical (quantum) capacitance of the graphene, and φ being determined by the geometrical capacitance C_G. In this article we consider the back gate for which [15] $V_{BG} \approx \varphi$, where $\varphi = ne/C_G$ is an electrostatic potential difference between the sheet and the gating electrode where $C_G = \varepsilon_d(0)/4\pi h$, $\varepsilon_d(0)$ is the dielectric constant of the dielectric. The approach which is used in this article can also be applied for the top gate. The radiative heat transfer is associated with the fluctuating electromagnetic field created by thermal fluctuations of the charge and current densities inside the bodies. In the case of a charged surface, thermal fluctuations of the surface displacement will also contribute to the fluctuating electromagnetic field and radiative heat transfer. The heat flux between two surfaces separated by a vacuum gap d, due to evanescent (non-radiative) electromagnetic waves (for which $q > \omega/c$) is determined by the formula [16–18]

$$J^{\text{rad}} = \int_0^\infty \frac{d\omega}{2\pi} \left[\Pi_g(\omega) - \Pi_d(\omega) \right]$$
$$\times \int \frac{d^2q}{(2\pi)^2} \frac{4 \operatorname{Im}R_d(\omega) \operatorname{Im}R_g(\omega) e^{-2qd}}{|1 - e^{-2qd}R_d(\omega)R_g(\omega)|^2}, \qquad (2)$$

$$\Pi_{g(d)}(\omega) = \frac{\hbar\omega}{e^{\hbar\omega/k_B T_{g(d)}} - 1},$$

$R_{g(d)}$ is the reflection amplitudes for the sheet (dielectric) for p-polarized electromagnetic waves.
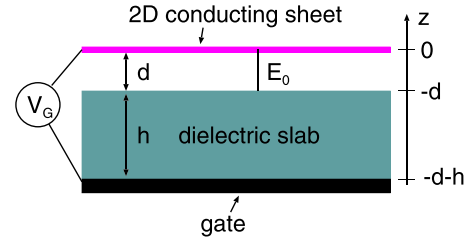

Figure 1. Schematic of the 2D device, in which the heat flux between a 2D sheet and a dielectric slab can be controlled by the potential difference.

To find the reflection amplitude for the charged sheet, write the electric field of the p-polarized electromagnetic wave in the non-retarded limit in the form:

$$\mathbf{E}(\mathbf{q}, \omega, z) = e^{i\mathbf{q}\cdot\mathbf{x} - i\omega t} \times \begin{cases} \mathbf{n}^+ e^{-qz} + R_p e^{qz}\mathbf{n}^-, z < 0 \\ T\mathbf{n}^+ e^{-qz}, z > 0 \end{cases} \qquad (3)$$

where $\mathbf{x} = (x, y)$, $\mathbf{q}$ is the wave vector in the (x, y)-plane, $\mathbf{n}^\pm = (\mp i\hat{q}, \hat{z})$. The electric field of the electromagnetic wave induces in the sheet the polarization

$$\mathbf{p}(\mathbf{x}, z) = (p_q\hat{q} + p_z\hat{z})\delta(z)e^{i\mathbf{q}\cdot\mathbf{x} - i\omega t} \qquad (4)$$

where p_q and p_z are the parallel and normal components of the surface dipole moment. The boundary condition for the normal component of the electric field can be obtained from the Maxwell equation

$$\nabla \cdot \mathbf{E} = \frac{dE_z}{dz} + iqE_q = -4\pi p_z\delta'(z) - 4\pi iqp_q\delta(z). \qquad (5)$$

Integrating (5) from -0 to $+0$, we get

$$E_z(z = +0) - E_z(z = -0) = -4\pi iqp_q, \qquad (6)$$

To obtain the boundary condition for the component of the electric field parallel to the surface, we calculate the circulation of $\mathbf{E}$ around the contour of the rectangle, two sides of which are parallel to the surface and located at $z = \pm 0$, and the other two sides are perpendicular to the surface. The magnetic induction field is continuous on the surface, so the magnetic flux through the area of the rectangle will be zero. Then from the Faraday's law it follows that [12, 19]

$$E_q(z = +0) - E_q(z = -0) = iq \int_{-0}^{+0} dz E_z(z)$$
$$= -iq \int_{-0}^{+0} dz z \frac{dE_z}{dz} = -4\pi iqp_z. \qquad (7)$$

The electromagnetic wave will create mechanical stress on the sheet $\tilde{\sigma}_{zi} = \sigma_{zi}(z = +0) - \sigma_{zi}(z = -0)$, where $\sigma_{zi}(z = \pm 0)$ is the Maxwell stress tensor at $z = \pm 0$, which in electrostatic limit has the form

$$\sigma_{ij} = \frac{1}{4\pi} \left(\tilde{E}_i\tilde{E}_j - \frac{1}{2}\delta_{ij}\tilde{\mathbf{E}} \cdot \tilde{\mathbf{E}} \right), \qquad (8)$$

where

$$\tilde{\mathbf{E}} = \mathbf{E} + \hat{z} \begin{cases} E_0', z > 0 \\ -E_0', z < 0 \end{cases} \quad (9)$$

where $E_0' = E_0/2 = 2\pi\sigma_g$ is the static electric field created by the surface charge density $\sigma_g = en$ on the sheet, $\mathbf{E}$ is the electric field of the electromagnetic wave, which is determined by (3). To linear order in the amplitude of the electromagnetic wave, the perpendicular component of the stress is determined by

$$\tilde{\sigma}_{zz} \approx \sigma_g \frac{E_z(+0) + E_z(-0)}{2}, \quad (10)$$

where $E_{z(q)}^{\pm} = E_{z(q)}(z = \pm 0)$. The stress $\tilde{\sigma}_{zz}$ produces a polarization of the sheet, with normal component of the dipole moment

$$p_z = \sigma_g u_z = \sigma_g^2 M_g \frac{E_z(+0) + E_z(-0)}{2}, \quad (11)$$

where M_g is the mechanical susceptibility of the sheet which determines the surface displacement of the sheet under an action of the stress $\tilde{\sigma}_{zz}$: $u_z = M_g \tilde{\sigma}_{zz}$. The stress $\tilde{\sigma}_{zq}$, which produces the polarization parallel to the surface of the sheet, is

$$\tilde{\sigma}_{zq} \approx ne \frac{E_q^+ + E_q^-}{2} \quad (12)$$

Thus, the polarization of graphene parallel to the surface arises due to the effective electric field $E_\parallel^{\mathrm{eff}} = (E_q^+ + E_q^-)/2$, which induces the sheet dipole moment $p_q = i\sigma(E_q^+ + E_q^-)/2\omega$ parallel to the surface, where σ is the sheet conductivity. The sheet conductivity can be expressed in terms of the dielectric function $\varepsilon_g = 1 + 2\pi iq\sigma/\omega$. From (3), (6) and (7), the boundary conditions can be written as

$$T - 1 - R = -(\varepsilon_g - 1)(T + 1 - R), \quad (13)$$

$$T - 1 + R = 2\pi q\sigma_g^2 M_g(T + 1 + R), \quad (14)$$

From (13) and (14) follows

$$R_g = \frac{\varepsilon_g - 1 + 2\pi q\sigma_g^2 M_g}{\varepsilon_g(1 - 2\pi q\sigma_g^2 M_g)}. \quad (15)$$

The reflection amplitude (15) has the resonances at $\mathrm{Re}\,\varepsilon_g = 0$ and $1 - 2\pi q\sigma_g^2\,\mathrm{Re}M_g = 0$ associated with the plasmon and phonon polaritons of the sheet, respectively. Close to the phonon polariton resonance

$$R_g \approx \frac{1}{1 - 2\pi q\sigma_g^2 M_g}. \quad (16)$$

Thus in this case the reflection amplitude depends only on M_g and does not depend on ε_g what means that at the phonon polariton resonance the optical properties of the sheet are determined only by the mechanical properties of the flexural mode. The reflection amplitude for the charged dielectric surface can be calculated in the same way as above for the sheet. Neglecting the polarization parallel to the surface, the boundary conditions on the surface of the dielectric can be written as

$$E_z(z = -d + 0) = \varepsilon_d(\omega)E_z(z = -d - 0), \quad (17)$$

$$E_q(z = -d + 0) - E_q(z = -d - 0) = -4\pi iqp_z^d, \quad (18)$$

where $\mathbf{E}(z > -d)$ determines the incident and reflected wave, and $\mathbf{E}(z < -d)$ is the refracted wave. For a constant electric field, the surface density of the polarization charge for the dielectric

$$\sigma_d = -\frac{\varepsilon_d(0) - 1}{\varepsilon_d(0)}\sigma_g, \quad (19)$$

where $\epsilon_d(\omega)$ is the dielectric function of a substrate, and $p_z^d = \sigma_d M_d E_z(d = -d + 0)$ is the dipole moment normal to the surface. From (17) and (18) the reflection amplitude for a charged dielectric surface is

$$R_d = \frac{\varepsilon_d - 1 + 4\pi q\sigma_d^2 M_d\varepsilon_d}{\varepsilon_d + 1 - 4\pi q\sigma_d^2 M_d\varepsilon_d}. \quad (20)$$

For metals $\sigma_g = -\sigma_d$, and in this case (20) is reduced to formula obtained in reference [12]. The reflection amplitude has resonance at

$$\mathrm{Re}[\varepsilon_d(1 - 4\pi q\sigma_d^2 M_d)] + 1 = 0. \quad (21)$$

For a polar dielectric, this resonance is associated with surface phonon polaritons arising from the hybridization of optical and acoustic waves. For small potential difference, when $2\pi q\sigma_g^2 M_g \ll 1$ and $4\pi q\sigma_d^2 M_d \ll 1$, the reflection amplitudes are determined by well-known formulas [18]

$$R_g = \frac{\varepsilon_g - 1}{\varepsilon_g}, \quad (22)$$

$$R_d = \frac{\varepsilon_d - 1}{\varepsilon_d + 1}. \quad (23)$$

2.2. Phonon heat transfer

2.2.1. van der Waals interaction between semi-infinite medium and a 2D sheet. In the case of the van der Waals interaction between a semi-infinite dielectric and a 2D sheet, such as graphene, the potential energy can be written as

$$U = C_2 \int d^2\mathbf{x}_1 \int d^2\mathbf{x}_2 \int_{-\infty}^{u_d(\mathbf{x}_1)} dz_1$$

$$\frac{1}{[(\mathbf{x}_1 - \mathbf{x}_2)^2 + (d + u_g(\mathbf{x}_2) - z_1)^2]^6}$$

$$\times -C_1 \int d^2\mathbf{x}_1 \int d^2\mathbf{x}_2 \int_{-\infty}^{u_d(\mathbf{x}_1)} dz_1$$

$$\frac{1}{[(\mathbf{x}_1 - \mathbf{x}_2)^2 + (d + u_g(\mathbf{x}_2) - z_1)^2]^3}, \quad (24)$$

where $u_d(\mathbf{x})$ and $u_g(\mathbf{x})$ are the surface displacements for the dielectric and sheet. Expanding (24) to second order in displacements, we get

$$U = \pi A\left(\frac{C_2}{45d^9} - \frac{C_1}{6d^3}\right) + \pi\left[\int d^2\mathbf{x}_1 u_d(\mathbf{x}_1) - \int d^2\mathbf{x}_2 u_g(\mathbf{x}_2)\right]$$

$$\times\left(\frac{C_2}{5d^{10}} - \frac{C_1}{2d^4}\right) + 6d\int d^2\mathbf{x}_1 \int d^2\mathbf{x}_2 u_d(\mathbf{x}_1)u_g(\mathbf{x}_2)$$

$$\times \left\{ \frac{C_1}{[(\mathbf{x}_1 - \mathbf{x}_2)^2 + d^2]^4} - \frac{2C_2}{[(\mathbf{x}_1 - \mathbf{x}_2)^2 + d^2]^7} \right\}$$

$$+ \pi \left(\frac{C_2}{d^{11}} - \frac{C_1}{d^5} \right) \left[\int d^2\mathbf{x}_1 u_d^2(\mathbf{x}_1) + \int d^2\mathbf{x}_2 u_2^2(\mathbf{x}_2) \right] + \cdots,$$

$$(25)$$

At the equilibrium distance the linear terms in the displacement vanish. Thus, the equilibrium distance $d_0 = (2C_2/5C_1)^{1/6}$. The stresses that act on surfaces of the dielectric and sheet, when they are displaced, are determined by

$$\sigma_d = -\frac{\delta U}{\delta u_d(\mathbf{x})} = -6dC_1 \int d^2\mathbf{x}_2 u_g(\mathbf{x}_2) \left\{ \frac{1}{[(\mathbf{x} - \mathbf{x}_2)^2 + d^2]^4} \right.$$

$$\left. - \frac{5d_0^6}{[(\mathbf{x} - \mathbf{x}_2)^2 + d^2]^7} \right\} - \frac{\pi C_1 u_d(\mathbf{x})}{d^5} \left[5\left(\frac{d_0}{d}\right)^6 - 2 \right],$$

$$(26)$$

$$\sigma_g = -\frac{\delta U}{\delta u_g(\mathbf{x})} = -6dC_1 \int d^2\mathbf{x}_2 u_d(\mathbf{x}_2) \left\{ \frac{1}{[(\mathbf{x} - \mathbf{x}_2)^2 + d^2]^4} \right.$$

$$\left. - \frac{5d_0^6}{[(\mathbf{x} - \mathbf{x}_2)^2 + d^2]^7} \right\} - \frac{\pi C_1 u_g(\mathbf{x})}{d^5} \left[5\left(\frac{d_0}{d}\right)^6 - 2 \right].$$

$$(27)$$

Using a Fourier transformation

$$u_i(\mathbf{x}) = \int \frac{d^2\mathbf{q}}{(2\pi)^2} u_i e^{i\mathbf{q}\cdot\mathbf{x}},$$

$$(28)$$

we get

$$\sigma_d = au_d - bu_g,$$

$$(29)$$

$$\sigma_g = au_g - bu_d,$$

$$(30)$$

where

$$a = \frac{\pi C_1}{d^5} \left[2 - 5\left(\frac{d_0}{d}\right)^6 \right],$$

$$(31)$$

$$b = \frac{\pi q^3 C_1}{4d^2} \left[K_3(qd) - \frac{q^3 d_0^6 K_6(qd)}{192d^3} \right],$$

$$(32)$$

where we have used that

$$\int d^2\mathbf{x}_1 \frac{u_1(\mathbf{x}_1)}{[(\mathbf{x}_1 - \mathbf{x})^2 + d^2]^{\mu+1}} = \int \frac{d^2\mathbf{q}}{(2\pi)^2} u_i e^{i\mathbf{q}\cdot\mathbf{x}} G_{\mu+1}(q),$$

$$(33)$$

$$G_{\mu+1}(q) = \int d^2\mathbf{x} \frac{e^{i\mathbf{q}\cdot\mathbf{x}}}{(r^2 + d^2)^{\mu+1}} = 2\pi \int_0^\infty \frac{J_0(qr)r dr}{(r^2 + d^2)^{\mu+1}}$$

$$= \frac{\pi}{2^{\mu-1}} \left(\frac{q}{d}\right)^\mu \frac{K_\mu(qd)}{\Gamma(\mu+1)}$$

$$(34)$$

where $K_\mu(z)$ is the Bessel function of the second kind and order μ (see reference [20]). For small argument the Bessel function can be approximated by formula [20]

$$K_\nu(z) \sim \frac{2^{\nu-1}\Gamma(\nu)}{z^\nu}$$

$$(35)$$

where $z \ll 1$. Using equation (35) it can be shown that for $qd \ll 1$ the 'spring' model [3] is valid for which $b = a = -K$, where K is a spring constant per unit area characterizing the interaction between the two solids [3]. At the equilibrium distance

$$a = -\frac{3\pi C_1}{d_0^5} = -K_0,$$

$$(36)$$

where K_0 is the spring constant at $d = d_0$. Thus the parameters of the interaction can be written in the form

$$a = \frac{K_0}{3} \left(\frac{d_0}{d}\right)^5 \left[2 - 5\left(\frac{d_0}{d}\right)^6 \right],$$

$$(37)$$

$$b = \frac{q^3 d_0^5 K_0}{12d^2} \left[K_3(qd) - \frac{q^3 d_0^6 K_6(qd)}{192d^3} \right].$$

$$(38)$$

2.2.2. Electrostatic interaction between dielectric surface and conducting 2D sheet. The electrostatic potential in the vacuum gap between the 2D sheet and dielectric has the form

$$\varphi = \sigma_g z + \text{const.}$$

$$(39)$$

The surface displacements of the sheet and dielectric

$$u_{zi}(\mathbf{x}) = u_i e^{i\mathbf{q}\cdot\mathbf{x}}$$

$$(40)$$

will give rise to normal component of surface dipole moments $p_{zi} = \sigma_i u_i$ resulting in a change of the electric field, which can be described by the potential

$$\phi(\mathbf{x}, z) = e^{i\mathbf{q}\cdot\mathbf{x}} \times \begin{cases} 0, & z > 0 \\ \nu_- e^{-qz} + \nu_+ e^{qz}, & -d < z < 0 \\ t e^{qz}, & z < -d \end{cases}$$

$$(41)$$

According to equations (17)–(19), on the dielectric surface at $z = -d$ the boundary conditions for the potential takes the form

$$v_+ e^{-qd} - v_- e^{qd} = \varepsilon_d(0)t e^{-qd},$$

$$(42)$$

$$v_+ e^{-qd} + v_- e^{qd} - t e^{-qd} = 4\pi \frac{\varepsilon_d(0) - 1}{\varepsilon_d(0)} \sigma_g u_d,$$

$$(43)$$

From equations (42)–(44) follows

$$\nu_- e^{qd} = -R_{d0}\nu_+ e^{-qd} - 4\pi\sigma_g u_d R_{d0},$$

$$(44)$$

where R_{d0} is determined by (23) at $\omega = 0$. Taking into account that in the electrostatic limit $\mathbf{E}(z) = 0$ for $z > 0$, from equation (7) follows the boundary condition at the surface of the sheet at $z = 0$

$$4\pi\sigma_g u_g + \nu_- + \nu_+ = 0.$$

$$(45)$$

The boundary condition (45) is the consequence of the requirement that the potential of the sheet should remain unchanged when the surface is displaced [14].

From (45) and (44)

$$\nu_+ = \frac{E_0}{1 - e^{-2qd}R_{d0}} \left(e^{-qd}R_{d0}u_d - u_g \right),$$

$$(46)$$

$$\nu_- = \frac{e^{-qd}R_{d0}E_0}{1 - e^{-2qd}R_{d0}}\left(e^{-qd}u_g - u_d\right). \qquad (47)$$

The electric field normal to the surfaces of the 2D sheet and dielectric for $-d < z < 0$ is

$$E_z = -E_0 + \frac{qE_0}{1 - e^{-2qd}R_d^0}\left[\left(e^{qz} + e^{-2qd}R_{d0}\,e^{-qz}\right)u_g - e^{-qd}\right.$$
$$\left. \times \left(e^{qz} + e^{-qz}\right)R_{d0}u_d\right]e^{\mathbf{q}\cdot\mathbf{x}}, \qquad (48)$$

and from Maxwell stress tensor, the stresses that act on the surfaces of the sheet and dielectric due to the surface displacements are

$$\sigma_g = K_g u_g - K u_d, \qquad (49)$$

$$\sigma_d = K_g u_d - K u_g, \qquad (50)$$

where

$$K_g = \frac{E_0^2}{4\pi}\frac{q\left(1 + e^{-2qd}R_{d0}\right)}{1 - e^{-2qd}R_{d0}}, \qquad (51)$$

$$K_d = \frac{E_0^2}{4\pi}\frac{qR_{d0}\left(1 + e^{-2qd}\right)}{1 - e^{-2qd}R_{d0}}, \qquad (52)$$

$$K = \frac{E_0^2}{2\pi}\frac{q\,e^{-qd}R_{d0}}{1 - e^{-2qd}R_{d0}}. \qquad (53)$$

2.2.3. Phonon heat flux between surfaces. The displacements of the surfaces $u_i = u_i^f + u_i^{ind}$, where u_i^f is the fluctuating displacement due to thermal and quantum fluctuations inside the bodies and u_i^{ind} is the induced displacement, which occurs due to the interaction between surfaces. Thus, according to equations (29), (30), (49) and (50) the displacements of the surfaces are determined by

$$u_g = u_g^f + M_g\sigma_g = u_g^f + M_g(K_g u_g - K u_d), \qquad (54)$$

$$u_d = u_d^f + M_d\sigma_d = u_d^f + M_d(K_d u_d - K u_g), \qquad (55)$$

where M_i is the mechanical susceptibility which determines the surface displacement under an action of the applied stress: $u_i^{ind} = M_i\sigma_i$, and where

$$K_g = \frac{E_0^2}{4\pi}\frac{q\left(1 + e^{-2qd}R_{d0}\right)}{1 - e^{-2qd}R_{d0}} + \frac{K_0}{3}\left(\frac{d_0}{d}\right)^5\left[2 - 5\left(\frac{d_0}{d}\right)^6\right], \qquad (56)$$

$$K_d = \frac{E_0^2}{4\pi}\frac{qR_{d0}\left(1 + e^{-2qd}\right)}{1 - e^{-2qd}R_{d0}} + \frac{K_0}{3}\left(\frac{d_0}{d}\right)^5\left[2 - 5\left(\frac{d_0}{d}\right)^6\right], \qquad (57)$$

$$K = \frac{E_0^2}{2\pi}\frac{q\,e^{-qd}R_{d0}}{1 - e^{-2qd}R_{d0}} + \frac{q^3 d_0^5 K_0}{12d^2}\left[K_3(qd) - \frac{q^3 d_0^6 K_6(qd)}{192d^3}\right]. \qquad (58)$$

According to the fluctuation–dissipation theorem, the spectral density of fluctuations of the surface displacements is determined by [21]

$$\langle|u_{g(d)}^f|^2\rangle = \hbar\,\mathrm{Im}M_{g(d)}(\omega, q)\coth\frac{\hbar\omega}{2k_{\mathrm{B}}T_{g(d)}}. \qquad (59)$$

From (54) and (55)

$$u_g = \frac{(1 - M_d K_d)u_g^f - M_g K u_d^f}{(1 - M_g K_g)(1 - M_d K_d) - K^2 M_g M_d}, \qquad (60)$$

u_d is obtained from u_g by the permutation of indexes $(g \leftrightarrow d)$. The mechanical stress that acts on the surface of the dielectric, due to fluctuations of the surface displacement of the sheet, is determined by

$$\sigma_{dg}^f = \frac{K u_g^f}{(1 - M_g K_g)(1 - M_d K_d) - K^2 M_g M_d}. \qquad (61)$$

The stress σ_{gd}^f can be obtained from σ_{dg}^f by the permutation $(g \leftrightarrow d)$. The heat flux from the sheet to dielectric due to the electrostatic and van der Waals interactions between the fluctuating surface displacements is [12, 21]

$$J^{\mathrm{ph}} = \langle\dot{u}_d^{\mathrm{ind}}\sigma_{dg}^f\rangle - \langle\dot{u}_g^{\mathrm{ind}}\sigma_{gd}^f\rangle$$
$$= 2\int_0^\infty\frac{d\omega}{2\pi}\int\frac{d^2q}{(2\pi)^2}\omega\left[\mathrm{Im}M_d\langle|\sigma_{dg}|^2\rangle - \mathrm{Im}M_g\langle|\sigma_{gd}|^2\rangle\right]$$
$$= \frac{1}{\pi^2}\int_0^\infty d\omega\left[\Pi_g(\omega) - \Pi_d(\omega)\right]$$
$$\times \int_0^\infty dq q\frac{K^2\,\mathrm{Im}M_g\,\mathrm{Im}M_d}{|(1 - K_g M_g)(1 - K_d M_d) - K^2 M_g M_d|^2}. \qquad (62)$$

In the 'spring' model [3] it is assumed that $K_g = K_d = -K$ and in this case (62) is reduced to

$$J_{\mathrm{spr}}^{\mathrm{ph}} = \frac{1}{\pi^2}\int_0^\infty d\omega\left[\Pi_g(\omega) - \Pi_d(\omega)\right]\int_0^\infty dq q\frac{K^2\,\mathrm{Im}M_g\,\mathrm{Im}M_d}{|1 + K(M_g + M_d)|^2}. \qquad (63)$$

3. Numerical results for graphene on a SiO$_2$ substrate

For an elastic sheet [22]

$$M_g = \frac{1}{\kappa q^4 - \rho\omega^2 - i\omega\rho\gamma}, \qquad (64)$$

where the bending stiffness of graphene $\kappa \approx 1$ eV, $\rho = 7.7 \times 10^{-7}$ kg m^{-2} is the surface mass density of graphene, γ is the damping constant for flexural motion of graphene which was estimated in reference [4] as

$$\gamma = \frac{\omega T}{100 T_{\mathrm{RT}}} \qquad (65)$$

where $T_{\mathrm{RT}} = 300$ K is the room temperature.

For an elastic semi-infinite medium the mechanical susceptibility M_d is determined by formula [23]

$$M_d = \frac{i}{\rho c_t^2}\left(\frac{\omega}{c_t}\right)^2\frac{p_l(q, \omega)}{S(q, \omega)}, \qquad (66)$$

where

$$S(q,\omega) = \left[\left(\frac{\omega}{c_t}\right)^2 - 2q^2\right]^2 + 4q^2 p_t p_l,$$

$$p_t = \left[\left(\frac{\omega}{c_t}\right)^2 - q^2 + i0\right]^{1/2}, \quad p_l = \left[\left(\frac{\omega}{c_l}\right)^2 - q^2 + i0\right]^{1/2},$$

where for SiO$_2$ the density $\rho = 2.65 \times 10^3$ kg m^{-3}, $c_l = 5968$ m s^{-1} and $c_t = 3764$ m s^{-1} are the longitudinal and transverse velocities of the acoustic waves.

The dielectric function of amorphous SiO$_2$ can be described using an oscillator model [24]

$$\varepsilon(\omega) = \epsilon_\infty + \sum_{j=1}^{2} \frac{\sigma_j}{\omega_{0,j}^2 - \omega^2 - i\omega\gamma_j}, \quad (67)$$

where parameters $\omega_{0,j}$, γ_j and σ_j were obtained by fitting the measured ε for SiO$_2$ to the above equation, and are given by $\epsilon_\infty = 2.0014$, $\sigma_1 = 4.4767 \times 10^{27}$ s^{-2}, $\omega_{0,1} = 8.6732 \times 10^{13}$ s^{-1}, $\gamma_1 = 3.3026 \times 10^{12}$ s^{-1}, $\sigma_2 = 2.3584 \times 10^{28}$ s^{-2}, $\omega_{0,2} = 2.0219 \times 10^{14}$ s^{-1}, and $\gamma_2 = 8.3983 \times 10^{12}$ s^{-1}.

In the numerical calculations we used the dielectric function of graphene, which was calculated within the random-phase approximation (RPA) [25, 26]. The dielectric function is an analytical function in the upper half-space of the complex ω-plane:

$$\varepsilon_g(\omega, q) = 1 + \frac{4k_F e^2}{\hbar v_F q} - \frac{e^2 q}{2\hbar\sqrt{\omega^2 - v_F^2 q^2}}$$

$$\times \left\{ G\left(\frac{\omega + 2v_F k_F}{v_F q}\right) - G\left(\frac{\omega - 2v_F k_F}{v_F q}\right) - i\pi \right\}, \quad (68)$$

where

$$G(x) = x\sqrt{x^2 - 1} - \ln(x + \sqrt{x^2 - 1}), \quad (69)$$

where the Fermi wave vector $k_F = (\pi n)^{1/2}$, n is the concentration of charge carriers, the Fermi energy $\epsilon_F = \hbar v_F k_F$, $v_F \approx 10^6$ m s^{-1} is the Fermi velocity.

For graphene on a SiO$_2$ substrate at equilibrium distance, according to density functional theory calculations, the spring constants [4] $K_0 = K_{OH} = 1.23 \times 10^{20}$ N m^{-3} and $K_0 = K_H = 1.56 \times 10^{20}$ N m^{-3} for the OH- and H-terminated SiO$_2$ substrate, which agrees rather well with estimation $K_0 = 1.82 \times 10^{20}$ N m^{-3} in reference [3]

Figure 2 shows the dependence of the heat flux between graphene and a SiO$_2$ substrate on the separation between them for different mechanisms and different free charge carries concentration n. The heat fluxes associated with the radiative and electrostatic phonon heat transfer have practically the same distance dependence and the difference between them decreases when the concentration n increases. The heat flux associated with the van der Waals interaction decays with distance much faster than for the radiative and electrostatic phonon heat transfer. Thus for $n_g > 10^{19}$m^{-2} the radiative and electrostatic phonon heat transfer dominate for practically all
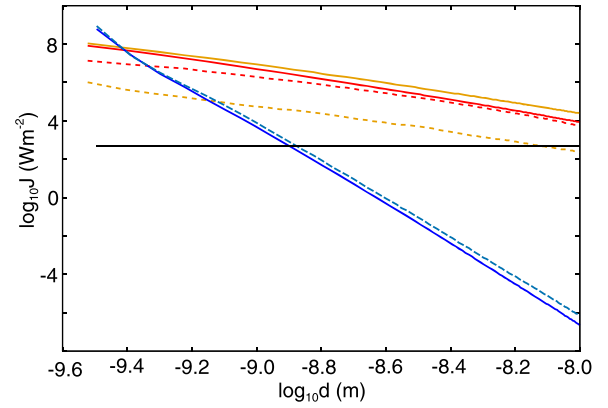

Figure 2. Dependence of the heat flux between graphene and a SiO$_2$ substrate on the separation between them for different mechanisms. The red and brown lines show the heat flux for the radiative and electrostatic phonon heat transfer: the solid and dashed lines for the concentration of the free charge carries in graphene $n_g = 10^{19}$m^{-2} and $n_g = 10^{18}$m^{-2}, respectively. The blue lines show the heat flux associated with the van der Waals interaction: the solid and dashed lines are for the nonlocal and local (the 'spring' model) theories of the van der Waals phonon heat transfer. The black line shows the radiative heat transfer associated with blackbody radiation.

separations. The blue solid and dashed lines show the contributions to the heat flux calculated using nonlocal and local theories of the van der Waals phonon heat transfer. For distances $d < 10$ nm the difference between these contributions is small, which confirms the validity of the 'spring' model for such distances.

Figure 3 shows the dependence of the heat flux associated with the radiative and electrostatic phonon heat transfer between graphene and a SiO$_2$ substrate on the concentration n_g at $d = 0.3$ nm (top) and $d = 1$ nm (bottom). In the SI units the potential difference φ between the gate and graphene is related with the concentration n_g by equation

$$\varphi = \frac{n_g e h}{\varepsilon_d(0)\varepsilon_0}. \quad (70)$$

The brown lines show only the contribution to the radiation heat flux due to fluctuations of the electronic polarization of graphene when the reflection amplitude is given by equation (22) while the pink line on top of figure 3 shows the radiation contribution from phonon polariton resonance associated with flexural mode of graphene when the reflection amplitude is given by equation (16). For the radiative heat transfer, for $n_g > 10^{18}$m^{-2} dominates the contribution which is associated with flexural modes of graphene. The sharp maximum in the radiative heat flux at $d = 0.3$ nm and $n_g \approx 6 \times 10^{18}$m^{-2} is related with the phonon polariton resonance. Estimation of one Π electron from one carbon atom leads to a surface charge density of about 8×10^{19}m^{-2}. Thus phonon polariton resonance can exist in graphene. In graphene, the interaction between flexural mode and in-plane mode are demonstrated to be weak [27, 28] which provide the foundation for separately modulating the thermal transport by flexural mode in graphene.
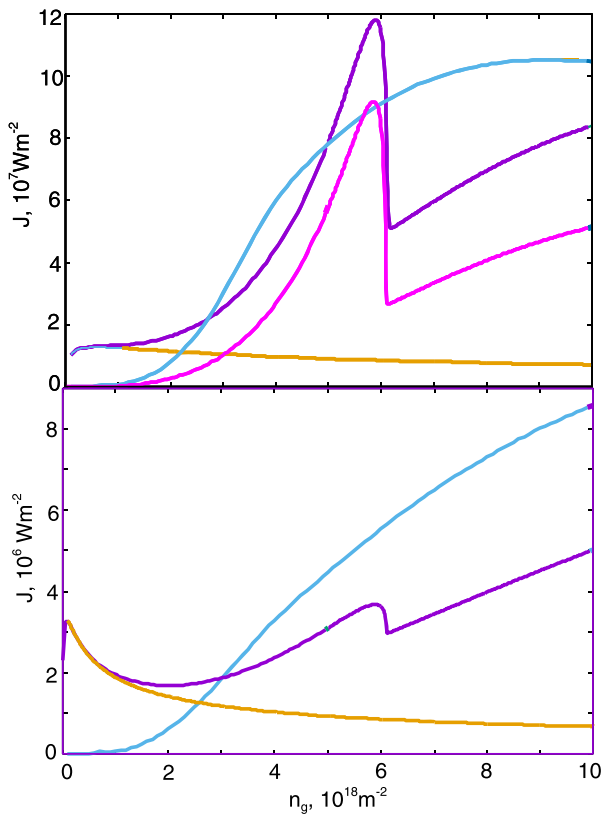
Figure 3. Dependence of the heat flux between graphene and a SiO_2 substrate on the concentration of the free charge carries in graphene. The violet and blue lines show the radiative and electrostatic phonon heat flux at $d = 0.3$ nm (top) and $d = 1$ nm (bottom). The brown lines show the radiative heat flux without contribution from the thermally fluctuating surface displacements, while the pink line on the top shows only these contributions.

4. Conclusion

The heat transfer between a 2D sheet and dielectric in presence of the gate voltage was calculated. The gate voltage induces a surface charge density on the sheet and dielectric. As a result, thermal fluctuations of the surface displacements create a fluctuating electromagnetic field that leads to an additional contribution to the radiative heat transfer. The phonon heat transfer due to the electrostatic and van der Waals interactions between surface displacements was calculated taking into account the nonlocality of these interactions. Numerical results are presented for the heat transfer between graphene and a SiO_2 substrate. It has been shown that, when the charge density $\sigma_g > 0.1 \, Cm^{-2}$ is induced on the graphene surface, the main contribution to the radiative heat transfer is associated with the flexural vibrational modes of graphene, and this contribution is of the same order and has the same distance dependence as the contribution from the electrostatic phonon heat transfer. Due to the strong distance dependence the van der Waals phonon heat transfer is only important for sub nanometer distances. For $\sigma_g > 1 \, Cm^{-2}$ the heat flux due to the radiative and electrostatic phonon heat transfer dominate for practically all distances. The obtained results can be important for the heat managements in the 2D devices.

References

[1] Ong Z-Y and Bae M-H 2019 Energy dissipation in van der Waals 2D devices *2D Mater.* **6** 032005
[2] Volokitin A I and Persson B N J 2011 Near-field radiative heat transfer between closely spaced graphene and amorphous SiO_2 *Phys. Rev.* B **83** 241407
[3] Persson B N J, Volokitin A I and Ueba H 2011 Phononic heat transfer across an interface: thermal boundary resistance *J. Phys.: Condens. Matter.* **23** 045009
[4] Ong Z-Y, Cai Y and Zhang G 2016 Theory of substrate-directed heat dissipation for single-layer graphene and other two-dimensional crystals *Phys. Rev.* B **94** 165427
[5] Li B, Wang L and Casati G 2006 Negative differential thermal resistance and thermal transistor *Appl. Phys. Lett.* **88** 143501
[6] Li N, Ren J, Wang L, Zhang G, Hnggi P and Li B 2012 Phononics: manipulating heat flow with electronic analogs and beyond *Rev. Mod. Phys.* **84** 1045
[7] Wang L and Li B 2007 Thermal logic gates: computation with phonons *Phys. Rev. Lett.* **99** 177208
[8] Ben-Abdallah P and Biehs S-A 2014 Near-field thermal transistor *Phys. Rev. Lett.* **112** 044301
[9] Ben-Abdallah P and Biehs S-A 2013 Phase-change radiative thermal diode *Appl. Phys. Lett.* **103** 191907
[10] Joulain K, Ezzahri Y, Drvillon J and Ben- Abdallah P 2015 Modulation and amplification of radiative far field heat transfer: towards a simple radiative thermal transistor *Appl. Phys. Lett.* **106** 133505
[11] Novoselov K S, Geim A K, Morozov S V, Jiang D, Zhang Y, Dubonos S V, Grigorieva I V and Firsov A A 2004 Electric field effect in atomically thin carbon films *Science* **306** 666
[12] Volokitin A I 2019 Effect of an electric field in the heat transfer between metals in the extreme near field *JETP Lett.* **109** 749
[13] Volokitin A I 2020 Contribution of the acoustic waves to near-field heat transfer *J. Phys.: Condens. Matter.* **32** 215001
[14] Pendry J B, Sasihithlu K and Craste R V 2016 Phonon-assisted heat transfer between vacuum-separated surfaces *Phys. Rev.* B **94** 075414
[15] Das A, Pisana S, Chakraborty B, Piscanec S, Saha S K, Waghmare U V, Novoselov K S, Krishnamurthy H R, Geim A K, Ferrari A C and Sood A K 2008 Monitoring dopants by Raman scattering in an electrochemically top-gated graphene transistor *Nat. Nanotechnol.* **3** 210
[16] Volokitin A I and Persson B N J 2001 Radiative heat transfer between nanostructures *Phys. Rev.* B **63** 205404
[17] Volokitin A I and Persson B N J 2007 Near field radiative heat transfer and noncontact friction *Rev. Mod. Phys.* **79** 1291
[18] Volokitin A I and Persson B N J 2017 *Electromagnetic Fluctuations at the Nanoscale. Theory and Applications* (Heidelberg: Springer)
[19] Langreth D C 1989 Macroscopic approach to the theory of reflectivity *Phys. Rev.* B **39** 10020

[20] Abramowitz M and Stegun I A 1970 *Handbook of Mathematical Functions* (New York: Dover)

[21] Landau L D and Lifshitz E M 1980 *Statistical Physics* (Course of Theoretical Physics vol 5) (Oxford: Pergamon)

[22] Landau L D and Lifshitz E M 1970 *Theory of Elasticity* (Course of Theoretical Physics vol 7) (Oxford: Pergamon)

[23] Persson B N J 2001 Theory of rubber friction and contact mechanics *Chem. Phys.* **115** 3840

[24] Chen D Z A, Hamam R, Soljacic M, Joannopoulos J D and Chen G 2007 Extraordinary optical transmission through subwavelength holes in a polaritonic silicon dioxide film *Appl. Phys. Lett.* **90** 181921

[25] Wunscvh B, Stauber T, Sols F and Guinea F 2006 Dynamical polarization of graphene at finite doping *New J. Phys.* **8** 318

[26] Hwang E H and Das Sarma S 2007 Dielectric function, screening, and plasmons in two-dimentional graphene *Phys. Rev.* B **75** 205418

[27] Sullivan S, Vallabhaneni A, Kholmanov I, Ruan X, Murthy J and Shi L 2017 Optical generation and detection of local nonequilibrium phonons in suspended graphene *Nano Lett.* **17** 2049

[28] An M, Song Q, Yu X, Meng H, Ma D, Li R, Jin Z, Huang B and Yang N 2017 Generalized two-temperature model for coupled phonons in nanosized graphene *Nano Lett.* **17** 5805